Received: 19 February 2019 | Accepted: 3 April 2019

DOI: 10.1111/cpr.12629

ORIGINAL ARTICLE

Cell Proliferation WILEY

Adipose tissue–derived stromal cells' conditioned medium modulates endothelial-mesenchymal transition induced by IL-1β/TGF-β2 but does not restore endothelial function

Tácia Tavares Aquinas Liguori[1,2] | Gabriel Romero Liguori[1,2] | Luiz Felipe Pinho Moreira[1] | Martin Conrad Harmsen[2]

[1]Laboratório de Cirurgia Cardiovascular e Fisiopatologia da Circulação (LIM-11), Faculdade de Medicina, Instituto do Coração (InCor), Hospital das Clinicas HCFMUSP, Universidade de Sao Paulo, Sao Paulo, Brazil

[2]Department of Pathology and Medical Biology, University of Groningen, University Medical Center Groningen, Groningen, The Netherlands

Correspondence
Martin Conrad Harmsen, Department of Pathology and Medical Biology, University of Groningen, University Medical Center Groningen, Hanzeplein 1 - EA11, 9713 GZ Groningen, the Netherlands.
Email: m.c.harmsen@umcg.nl

Abstract

Objectives: Endothelial cells undergo TGF-β–driven endothelial-mesenchymal transition (EndMT), representing up to 25% of cardiac myofibroblasts in ischaemic hearts. Previous research showed that conditioned medium of adipose tissue–derived stromal cells (ASC-CMed) blocks the activation of fibroblasts into fibrotic myofibroblasts. We tested the hypothesis that ASC-CMed abrogates EndMT and prevents the formation of adverse myofibroblasts.

Materials and methods: Human umbilical vein endothelial cells (HUVEC) were treated with IL-1β and TGF-β2 to induce EndMT, and the influence of ASC-CMed was assessed. As controls, non-treated HUVEC or HUVEC treated only with IL-1β in the absence or presence of ASC-CMed were used. Gene expression of inflammatory, endothelial, mesenchymal and extracellular matrix markers, transcription factors and cell receptors was analysed by RT-qPCR. The protein expression of endothelial and mesenchymal markers was evaluated by immunofluorescence microscopy and immunoblotting. Endothelial cell function was measured by sprouting assay.

Results: IL-1β/TGF-β2 treatment induced EndMT, as evidenced by the change in HUVEC morphology and an increase in mesenchymal markers. ASC-CMed blocked the EndMT-related fibrotic processes, as observed by reduced expression of mesenchymal markers *TAGLN* ($P = 0.0008$) and *CNN1* ($P = 0.0573$), as well as SM22α ($P = 0.0501$). The angiogenesis potential was impaired in HUVEC undergoing EndMT and could not be restored by ASC-CMed.

Conclusions: We demonstrated that ASC-CMed reduces IL-1β/TGF-β2-induced EndMT as observed by the loss of mesenchymal markers. The present study supports the anti-fibrotic effects of ASC-CMed through the modulation of the EndMT process.

Tácia Tavares Aquinas and Gabriel Romero Liguori equally contributed to the manuscript.

1 | INTRODUCTION

Heart failure (HF) is an irreversible and potentially lethal clinical condition that affects nearly 23 million people worldwide.[1] The five-year survival is approximately 50%. Obviously, HF impacts significantly on the quality of life and is an increasing burden on society and health care. Heart failure presents as various forms of idiopathic or heritable cardiomyopathy and as the consequence of adverse cardiac tissue remodelling after acute myocardial infarction.

In normal physiology, cardiac tissue is in homeostasis that is maintained by a well-regulated biochemical and biomechanical crosstalk between the parenchyma and the supportive tissue stroma. Cardiac parenchyma comprises cardiomyocytes, while the stroma consists of vasculature, fibroblasts and their product, the extracellular matrix (ECM). The ECM provides structural support and architecture and instructs adhered tissue cells.[2] HF disrupts the cardiac tissue homeostasis. A prominent feature is the proliferation of myofibroblasts and their excessive deposition and accumulation of fibrotic ECM. Thus, HF is a process of cardiac fibrosis. Differentiation of cardiac fibroblasts to myofibroblasts is a major contribution to HF.[3,4] Several other cell types, both endogenous in the heart and exogenous, also contribute to cardiac fibrosis.[5] The heart is particularly rich in capillaries and thus endothelial cells. Under pathological conditions, endothelial cells contribute to adverse wound healing and tissue remodelling via endothelial-mesenchymal transition (EndMT) and contribute significantly to cardiac fibrosis and development of heart failure.[6,7] After acute myocardial infarction in mice, up to 25% of cardiac myofibroblasts are the consequence of EndMT.[8] Irrespective of the source, *for example*, fibroblasts or endothelial cells, the resulting myofibroblasts are indistinguishable with respect to proliferation and ECM remodelling. Interestingly, EndMT is pivotal during cardiogenesis, when EndMT underlies the development of heart valves.[9] In contrast, in adult life, EndMT is related to pathophysiological phenomena such as cardiac fibrosis,[10-12] after myocardial infarction,[8,13] diabetic cardiomyopathy[14,15] and hypertensive heart disease.[11,16] Therefore, inhibition or reversal of cardiac EndMT is a therapeutic option to interfere with heart failure.

Endothelial-to-mesenchymal transition is a relatively slow de-differentiation process (days to weeks) that is driven by pro-fibrotic growth factors of the TGF-ß superfamily,[17,18] such as TGF-β2. Several processes coincide: endothelial cells loose cell-to-cell contacts and the downregulated endothelial markers. This causes the cells to transit from their characteristic cobblestone morphology to a spindle-like shape. Simultaneously, a progressive upregulation of mesenchymal markers occurs, such as smooth muscle protein 22 alpha (SM22α), calponin and alpha-smooth muscle actin (αSMA). Similar to myofibroblasts, the EndMT process renders cells highly migratory and proliferative, while these become resistant to apoptosis too. The process of EndMT also coincides with the increased production and deposition of extracellular matrix, which contributes to the development and progression of cardiac fibrosis including the increased stiffness of the failing heart.[19,20]

The TGF-β superfamily is important during embryogenesis, but also for wound healing, and thus influences cell growth, proliferation, differentiation and migration.[21] In addition, TGF-β members are strong regulators of ECM remodelling, in particular, through upregulation of constructive proteins such as collagens. All three TGF-β isoforms stimulate EndMT.[22-28] In cardiovascular wound healing, fibrosis coincides with inflammation. In fact, EndMT is synergized by TGF-β2 and IL-1β.[29,30] Heart failure is also associated with pro-fibrotic stimuli by members of the TGF-β superfamily, inflammation and reactive oxygen species (ROS). These three triggers are tightly interrelated because TGF-ß promotes inflammatory activation via TAK1, similar to ROS, and with it, EndMT.[31] We have shown that pro-fibrotic stimuli and pro-inflammatory stimuli synergize EndMT,[29,30] and other studies showed that ROS mediates the EndMT process through the TGF-β superfamily.[32,33]

Cardiac stem cell therapy with mesenchymal stem/stromal cells (MSC) has shown to improve remodelling after acute myocardial infarction. This suggests that MSC affect myofibroblast formation and function. The intramyocardial administration of mesenchymal stromal cells (MSC), which include adipose tissue–derived stromal cells (ASC), has benefit for cardiac function and remodelling in a variety of cardiac diseases.[34-42] As a matter of fact, injection of conditioned medium of MSC (CMed) also improved cardiac function.[43,44] Previous research in our laboratory showed that ASC secrete paracrine factors that abrogate TGF-β–induced differentiation of dermal fibroblasts to myofibroblasts which is a mesenchymal transition too.[45] In general, ASC and their secreted bioactive factors harbour pro-regenerative [46-48] and anti-inflammatory potential.[49,50] In addition, ASC promote angiogenesis. Therefore, we hypothesized that the formation of myofibroblasts from endothelial cells via EndMT, which also is a TGF-β–driven process and synergized by IL-1β, is down-modulated by the paracrine action of ASC while it would rescue their endothelial phenotype. We tested our hypothesis in vitro, by assessing the influence of adipose tissue–derived stromal cells' conditioned medium (ASC-CMed) on pro-fibrotic and pro-inflammatory–induced EndMT.

2 | EXPERIMENTAL

2.1 | Cell sources, cell culture, conditioned medium and experimental groups

Human umbilical vein endothelial cells (HUVEC) were obtained from the endothelial cell culture facility of our institution and comprised pools of at least three donors. Cells were seeded on gelatin-coated plates (1% gelatin solution in PBS) at a density of 35 000 cells/cm^2 and cultured until confluency in endothelial cell medium (ECMed) composed of RPMI 1640 basal medium (#BE04-558F, Lonza) with 10% heat-inactivated foetal bovine serum (FBS; #F0804, Sigma-Aldrich), 1% penicillin/streptomycin (#15140122, Gibco Invitrogen), 1% L-glutamine (#17-605E, Lonza BioWhittaker), 5 U/mL heparin (LEO Laboratories Limited) and 50 μg/mL bovine brain extract (BBE, home-made preparation). HUVEC between passages 3 and 6 were used for the experiments. Confluent HUVEC were divided into six groups with

TABLE 1 Experimental groups

Group	Description
ECMed	HUVEC culture only with endothelial cell medium
ECMed/IL-1β	HUVEC culture with endothelial cell medium added with IL-1β
ECMed/IL-1β/TGF-β2	HUVEC culture with endothelial cell medium added with IL-1β and TGF-β2
ASC-CMed	HUVEC culture only with ASC conditioned media
ASC-CMed/IL-1β	HUVEC culture with ASC conditioned media added with IL-1β
ASC-CMed/IL-1β/TGF-β2	HUVEC culture with ASC conditioned media added with IL-1β and TGF-β2

ASC, adipose tissue-derived stromal cells; ASC-CMed, conditioned media from adipose tissue-derived stromal cells; ECMed, endothelial culture medium; IL-1β, human recombinant interleukin-1 beta; TGF-β2, human transforming growth factor beta 2; UVEC, human umbilical vein endothelial cells.

different induction/ASC-CMed combinations, as described in Table 1, and cultured for 5 days. Human recombinant interleukin-1β (IL-1β; #200-01B, PeproTech) and human transforming growth factor beta 2 (TGF-β2; #100-35B, PeproTech) were used to stimulate the EndMT process at a concentration of 10ng/mL in all experiments.

Human ASC were isolated as described previously.[51] Briefly, human abdominal fat was obtained by liposuction. Tissue was washed with phosphate-buffered saline (PBS) and then enzymatically digested with 0.1% collagenase A (#11088793001, Roche Diagnostic, Mannheim, Germany) in PBS with 1% bovine serum albumin (BSA; #A9647, Sigma-Aldrich). The tissue was shaken constantly at 37°C for 2 hours. After this, the digested tissue was washed in 1% BSA in PBS and filtered using 70 μm cell strainers. The filtered suspension was centrifuged at 600 ***g*** for 10 minutes, and the cell pellet was resuspended in lysis buffer containing ammonium chloride to remove red blood cells, centrifuged again and resuspended in Dulbecco's modified Eagle's medium (DMEM; #12-604F, Lonza) with 10% foetal bovine serum (FBS; #F0804, Sigma-Aldrich), 1% penicillin/streptomycin (#15140122, Gibco Invitrogen) and 1% L-glutamine (#17-605E, Lonza BioWhittaker). Cells were cultured at 37°C in a humidified incubator with 5% CO_2. The medium was refreshed every 2 days. Cells were passed at a ratio of 1:3 after reached confluency. The characterization of the cells was routinely performed as previously described by our group and confirmed the required marker pattern and biological behaviour of ASC.[52]

After the second passage, ASC were maintained in ECMed. ASC-CMed was obtained from confluent cultures of ASC between passages 3 and 6 from 3 different donors. For ASC-CMed, cells were cultured in ECMed and the conditioned medium was harvested after 48 hours, filtered in 0.22 μm filters and stored at −20°C until use. The expression of fibroblast growth factor 1 (FGF-1) and vascular endothelial growth factor (VEGF) was determined in the medium collected from ASC. For this purpose, Magnetic Luminex Human Premixed Multi-Analyte Kit (R&D Systems) was used according to the manufacturer's protocol. DMEM only was used as negative control.

2.2 | Immunofluorescence, Gene Expression and Immunoblotting

2.2.1 | Immunofluorescence

HUVEC were cultured in 96-well tissue culture plates in ECMed. After 5 days of EndMT induction, cells were fixed at room temperature with 2% paraformaldehyde (PFA) for 30 minutes. Cells were permeabilized with 1% Triton-X 100 in PBS at room temperature for 15 minutes and blocked with 5% donkey serum in PBS and 1% BSA at room temperature for 15 minutes. Subsequently, cells were incubated with primary antibodies diluted in 5% donkey serum in PBS at room temperature for 2 hours. The following primary antibodies were used: rabbit anti-SM22α (1:400; #ab14106, Abcam) and mouse anti-human PECAM-1 (1:200; #MAB9381, R&D Systems, Oxon). Controls were incubated with 5% donkey serum in PBS instead of primary antibody. Next, cells were washed with 0.05% Tween-20 in PBS and incubated with secondary antibodies in 5% donkey serum in PBS with 4',6-diamidino-2-phenylindole (DAPI; 1:5000; #D9542-5MG, Sigma-Aldrich) and Alexa Fluor® 488 phalloidin (1:400; #A12379, Life Technologies) at room temperature for 1 hour. The following secondary antibodies were used: donkey anti-rabbit IgG (H + L) Alexa Fluor® 594 (1:400; #A-21207, Life Technologies) and donkey anti-mouse IgG (H + L) Alexa Fluor® 594 (1:400; #ab150108, Abcam). Finally, cells were washed three times with PBS and the plates were imaged with EVOS FL System (Thermo Fisher Scientific) using Texas Red (TXR), DAPI and Green Fluorescent Protein (GFP) channels with 20× magnification.

2.2.2 | Gene expression analysis

HUVEC were cultured in 75 cm^2 flasks. After 5 days of induction, total RNA was isolated using TRIzol reagent (#15596018, Invitrogen Corp) according to the manufacturer's protocol. RNA concentration and purity were determined using a NanoDrop Spectrophotometer (Thermo Scientific). Between 300 ng and 5000 ng of total RNA was used for cDNA synthesis, which was performed using RevertAid™ First Strand cDNA Synthesis Kit (Thermo Fisher Scientific) according to the manufacturer's protocol. The cDNA equivalent of 12 ng total RNA was used per single qPCR. PCR was performed using SYBR Green (Bio-Rad, Hercules) with the ViiA7 Real-Time PCR System (Applied Biosystems). Each analysis was done in duplicate for each one of the independent experiments. The primers used are listed in Table S1. Data were analysed using ViiA7 software (Applied Biosystems) and normalized with the ΔC_t method, using the geometrical mean of 18S ribosomal RNA (*18S RNA*) cycle threshold (C_T) values. The fold-change in gene expression vs the no treatment control group (ECMed) was calculated using the $\Delta\Delta C_T$ method.

2.2.3 | Immunoblotting analysis

HUVEC were cultured in 75 cm^2 flasks. After 5 days of induction, cells were rinsed with ice-cold PBS and lysed in 100 μL of ice-cold lysis buffer (RIPA; #89900, Thermo Fisher Scientific) containing 1% protease inhibitor cocktail (PIC; #P8340, Sigma-Aldrich) and 1% Halt™ Phosphatase Inhibitor Cocktail (#78420, Thermo Fisher Scientific). The lysed cells were collected in 2 mL microcentrifuge tubes, and the contents were homogenized by sonication at 30 W for 30 seconds and centrifuged at 7500 ***g*** at 4°C for 5 minutes. The supernatant was collected for the protein concentration determination using the Bio-Rad DC Protein Assay (#5000112; Bio-Rad, Hercules) according to the manufacturer's protocol. Gels (12%) were loaded with 25-30 μg of protein per lane. After electrophoresis, gels were blotted onto nitrocellulose membranes (#170-4270; Bio-Rad, Hercules). Blots were blocked with Odyssey® Blocking Buffer (#927-40000, LI-COR, Lincoln) in a dilution of 1:1 with PBS at 4°C overnight. Afterwards, blots were incubated with the primary antibodies overnight. The following primary antibodies were used: rabbit anti-SM22α (1:1000; #ab14106, Abcam), rabbit anti–VE-cadherin (1:500; #2500S, Cell Signalling), and mouse anti-GAPDH (1:1000; #ab9484, Abcam). Then, the membranes were washed with Tris-buffered saline (TBS) with 0.1% Tween-20 (TBST) 30 minutes and incubated with the Odyssey® secondary antibodies goat anti-rabbit IRDye 680LT (1:10000; #926-68021, LI-COR, Lincoln) and goat anti-mouse IRDye 800CW (1:10,000; #926-32210, LI-COR, Lincoln) for 1 hour. Non-bound secondary antibodies were removed by washing with TBST for 30 minutes. Then, blots were washed with TBS for 5 minutes and scanned with Odyssey® Infrared Imaging System (LI-COR, Lincoln).

2.2.4 | Endothelial sprouting assay

HUVEC were cultured in 25 cm^2 flasks. After 5 days of induction, cells were detached from the flasks and counted, and, for each group, 15 000 cells were resuspended in 50 μL of ECMed. Subsequently, cells were seeded in wells of a μ-Slide Angiogenesis Plate (Ibidi GmbH) previously coated and incubated at 37°C with 10 μL of Matrigel® (#356231, BD Biosciences) for 2 hours. The sprouting was allowed to proceed for 8 hours. Every condition was done in duplicate, and the experiment was performed three times independently. Formation of sprouting networks was imaged with a DM2000 LED Inverted Microscope (Leica) using 2.5× magnification and analysed using ImageJ software. The number of nodes, branches, segments, total length, number of meshes and mean mesh size were analysed.

2.3 | Statistical analysis

All data were obtained from at least three independent experiments performed in duplicate. Data are presented as the mean ± SE of the mean (SEM). Graphs and statistical analysis were done using GraphPad Prism (version 6.01; GraphPad Software, Inc). Differences among multiple groups were analysed by one-way ANOVA with Sidak's multiple comparison test for the two groups of interested in each scenario.

3 | RESULTS

3.1 | ASC secrete fibroblast growth factor 1 (FGF-1) and vascular endothelial growth factor (VEGF)

The growth factor release from ASC was determined by the measurement of FGF-1 and VEGF, in the medium collected from the cells, using the Magnetic Luminex Human Premixed Multi-Analyte Kit. The concentration of growth factors was 21.7 ± 0.7 pg/mL for FGF-1 and 95.6 ± 3.1 pg/mL for VEGF. DMEM only showed growth factor concentrations close to zero (Figure 1).

3.2 | HUVEC undergoing EndMT present conformational changes

All cells started the experiment as a cobblestone morphology (Figure 2). After two days, the cells receiving inflammatory stimuli had disrupted intercellular adhesions. During this same period, co-stimulation with pro-inflammatory and pro-fibrotic factors, that is, induction of EndMT, part of the HUVEC showed more pronounced disruption of intercellular adhesions and had altered from their characteristic cobblestone morphology into spindle-shaped cells (Figure 2). The cells cultured with ASC-CMed retained their cobblestone morphology, but it did not inhibit the disruption of intercellular adhesions, in the cells neither with only inflammatory stimulation nor with both inflammatory and pro-fibrotic stimulation (Figure 2). Control cells kept their morphology for the entire duration of the experiment. The inflammatory environment did not change the cells compared to the second day. In EndMT-induced HUVEC, all intercellular adhesions were disrupted, while all cells were spindle-shaped at day 5 (Figure 2). Although these changes could be seen both in the groups cultured only with IL-1β and those

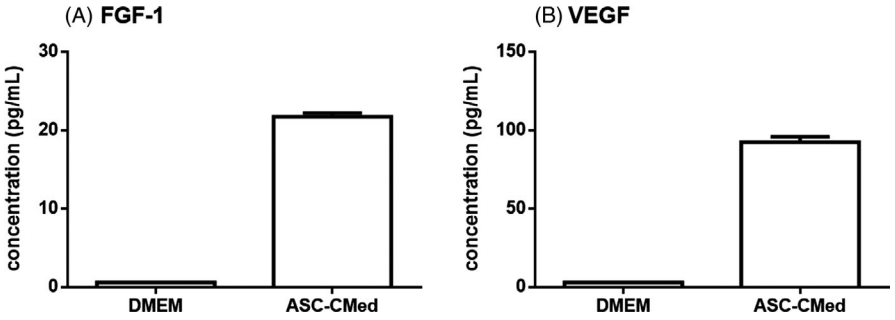

FIGURE 1 Concentration of growth factors released by ASC in the conditioned medium. A, FGF-1 B, VEGF

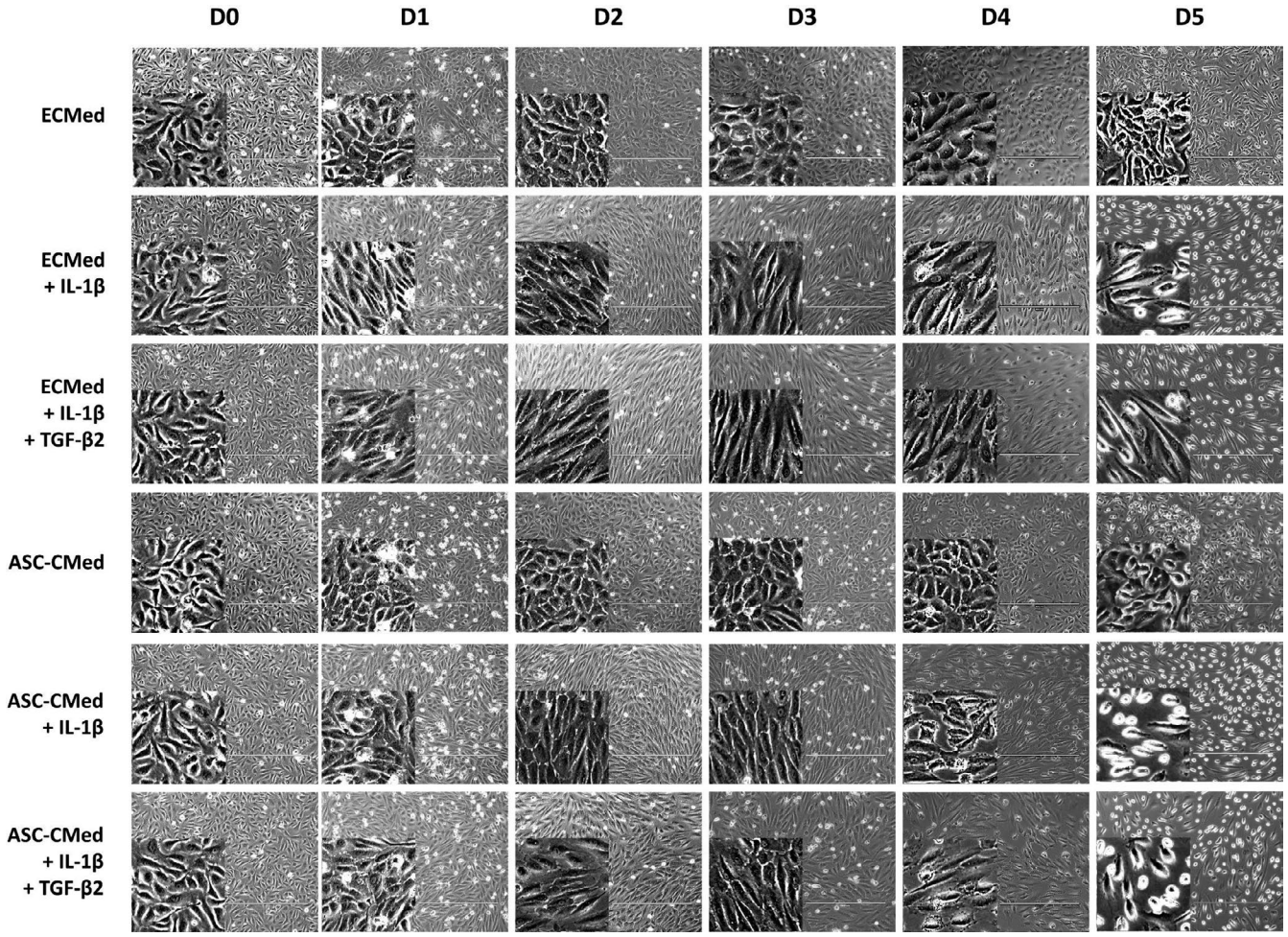

FIGURE 2 Conformational changes in HUVEC under stimulation with IL-1β or co-stimulation with IL-1β/TGF-β2, both in ECMed and in ASC-CMed, for five days. Scale reference: 400 μm

undergoing co-stimulation with IL-1β and TGF-β2, the latter showed a more explicit transformation. The use of ASC-CMed did not prevent cell-to-cell adhesion disruption or morphology changes to occur.

3.3 | Inflammatory gene expression in activated HUVEC is refractory to ASC-secreted factors

Pro-inflammatory stimulation of HUVEC with IL-1β upregulated expression of *IL8*, *ICAM1* and *VCAM1*, which encode respectively chemoattractant and adhesion molecules required for endothelial transmigration of activated leucocytes (Figure 3). This upregulation was refractory to simultaneous treatment with ASC-CMed (Figure 3). Also, IL-1β stimulation upregulated expression of two pro-inflammatory cytokine genes, *IL1B* and *IL6*, which was unaffected by ASC-CMed, except for *IL6* that was slightly upregulated by ASC-CMed (one-way ANOVA, $P = 0.0075$; Sidak's multiple comparison test, $P = 0.0683$). The influence of TGF-β2 on IL-1β–stimulated HUVEC was negligible with respect to the expression of these inflammatory activation-related genes, neither did co-stimulation with ASC-CMed affect these genes. However, the expression of *IL6* was normalized compared to stimulation of HUVEC with IL-1ß and ASC-CMed.

3.4 | Mesenchymal gene expression in EndMT-induced HUVEC is suppressed by ASC-secreted factors while extracellular matrix genes are not

Pro-inflammatory stimulation of HUVEC with IL-1β did not change the expression of *PECAM1* and *CDH5* (Figure 4A-B) which are endothelial intercellular adhesion molecules that support the maintenance of the endothelial barrier. As expected, this pro-inflammatory activation abolished eNOS (*NOS3)* gene expression (Figure 4C). Similarly, endothelial co-stimulation with IL-1β and TGF-β2 did not affect the expression of *PECAM1* and *CDH5*, while *NOS3* expression was abolished too (Figure 4A-C). Though TGF-β2 has anti-inflammatory effects, it could not alleviate the strong influence of IL-1β on *NOS3* downregulation. The expression of these endothelial-specific genes was unaffected by ASC-CMed neither in unstimulated controls nor after cytokine activation (Figure 4A-C). The expression of *TAGLN* and *CCN1*, mesenchymal genes typical for EndMT, was unaffected in HUVEC after pro-inflammatory stimulation (Figure 4D-E). As expected, co-stimulation with IL-1ß and TGF-ß2 upregulated expression of *TAGLN* and *CCN1*. Endothelial gene expression (*PECAM1*, *CDH5*, and *NOS3*) was not

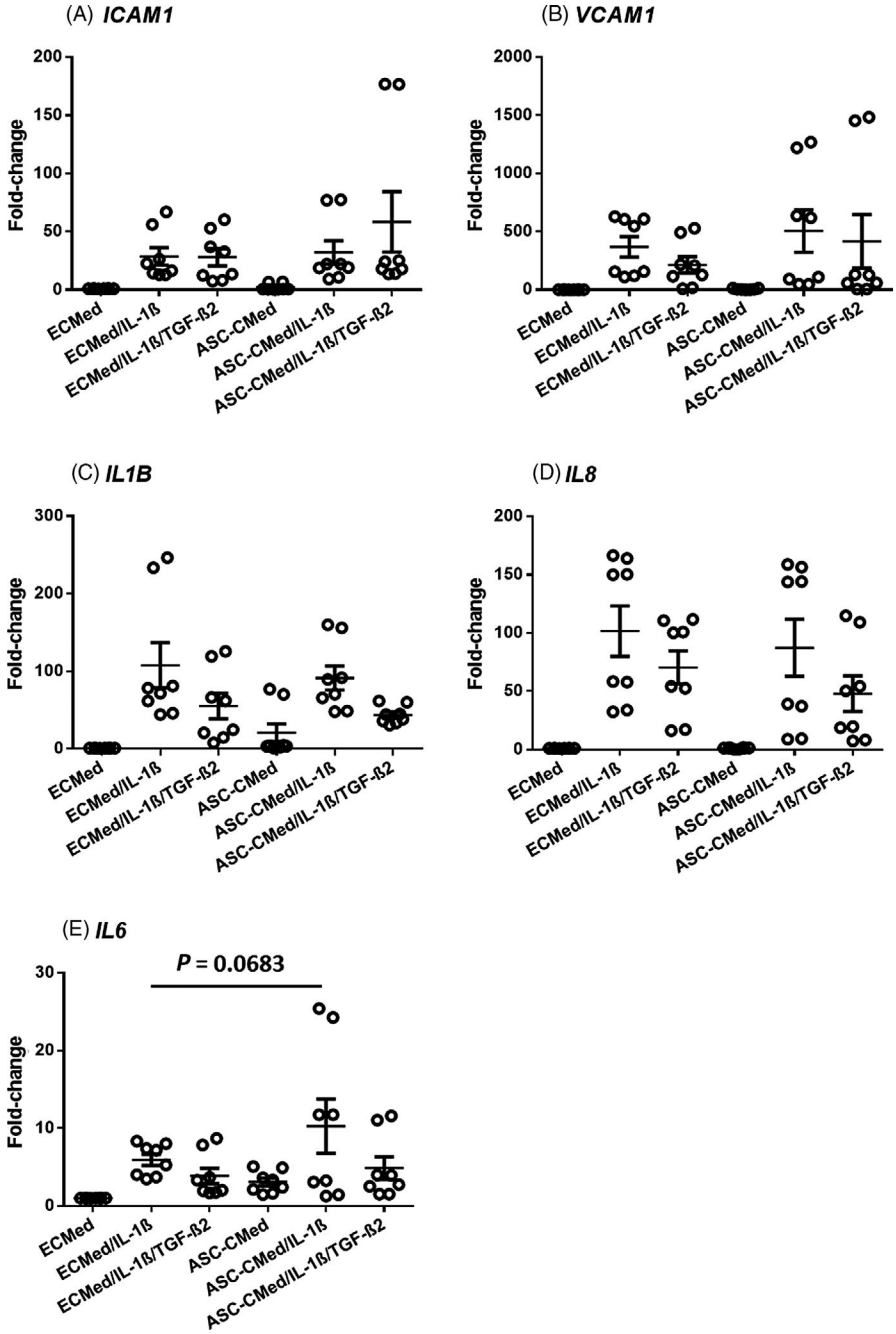

FIGURE 3 Gene expression (mRNA) of inflammatory markers A, *ICAM1*, B, *VCAM1*, C, *IL1B*, D, *IL8*, and E, *IL6* by semi-quantitative RT-qPCR of HUVEC after stimulation with IL-1β or co-stimulation with IL-1β/TGF-β2, both in ECMed and in ASC-CMed, for five days. Data were analysed by one-way ANOVA with Sidak's multiple comparison test for the groups ECMed/IL-1β vs ASC-CMed/IL-1β; *P*-values for the Sidak's multiple comparison test are shown in the figure. Values represent mean ± SEM of 4 independent experiments in duplicate

affected by ASC-CMed in controls or cytokine-stimulated HUVEC. On the other hand, ASC-CMed normalized expression of *TAGLN* (Figure 4D, one-way ANOVA, $P < 0.0001$; Sidak's multiple comparison test, $P = 0.0008$) and, albeit to a lesser extent, of *CCN1* (Figure 4E, one-way ANOVA, $P = 0.0976$; Sidak's multiple comparison test, $P = 0.0573$) in HUVEC that were induced to undergo EndMT, that is, co-stimulation with IL-1β and TGF-β2 (Figure 4D-E). Over the five-day period of the pro-inflammatory induction or the induction of EndMT, the expression of representative fibrosis-related extracellular matrix genes *COL1A1* and *COL3A1* was upregulated after co-stimulation with both cytokines (Figure 4F-G). In contrast to the structural mesenchymal genes *TAGLN* and *CCN1*, the upregulation of *COL1A1* and *COL3A1* was refractory to treatment with ASC-CMed (Figure 4F-G).

To corroborate the gene expression results, protein expression was assessed by immunoblotting of the endothelial marker VE-cadherin (CD144, *CDH5* gene) and the mesenchymal marker SM22 (transgelin, *TAGLN* gene) (Figure 5). The expression of both proteins did not change in upon pro-inflammatory stimulation, nor was it affected by co-treatment with ASC-CMed. The expression of VE-cadherin, however, was slightly increased by ASC-CMed, irrespective of cytokine treatment (Figure 5A, one-way ANOVA, $P = 0.1990$; Sidak's multiple comparison test, $P = 0.0673$). The upregulated expression of SM22 after stimulation with both cytokines was suppressed by ASC-CMed

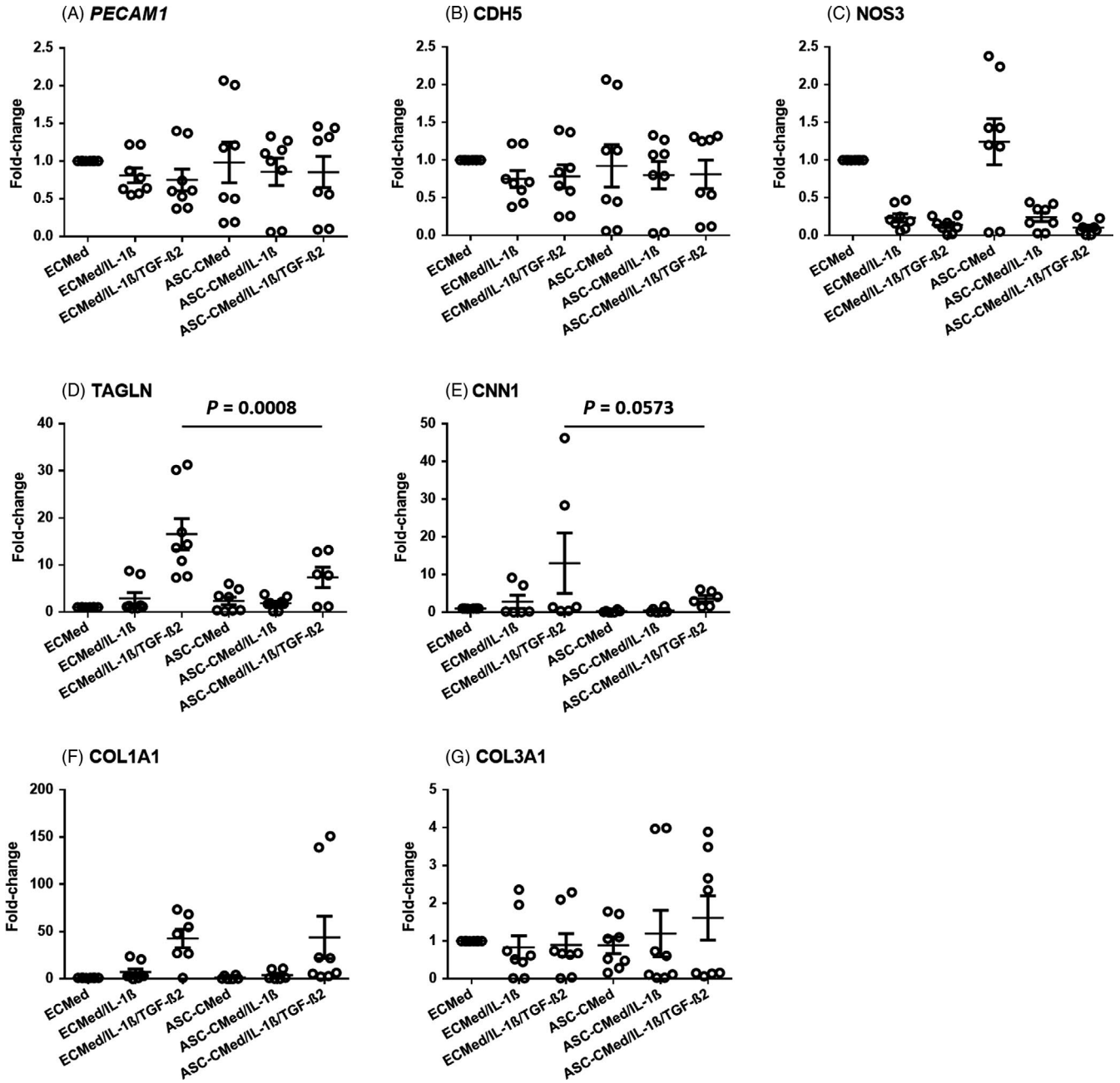

FIGURE 4 Gene expression (mRNA) of endothelial markers A, *PECAM1*, B, *CDH5* and C, *NOS3*; mesenchymal markers D, *TAGLN* and E, *CNN1;* and collagens F, *COL1A1* and G, *COL3A1* by semi-quantitative RT-qPCR of HUVEC under stimulation with IL-1β or co-stimulation with IL-1β/TGF-β2, both in ECMed and in ASC-CMed, for five days. Data were analysed by one-way ANOVA with Sidak's multiple comparison test for the groups ECMed/IL-1β/TGF-β2 vs ASC-CMed/IL-1β/TGF-β2; *P*-values for the Sidak's multiple comparison test are shown in the figure. Values represent mean ± SEM of four independent experiments in duplicate

(Figure 5B, one-way ANOVA, $P = 0.0064$; Sidak's multiple comparison test, $P = 0.0501$).

Immunofluorescence staining for the endothelial marker PECAM (CD31) showed that none of the cytokine treatments, nor the co-treatment with ASC-CMed, affected its expression (Figure 6, top row panels). In contrast to immunoblotting, in situ immunostaining of SM22α proved less sensitive, yet it was detectable after stimulation with IL-1β alone or together with TGF-β2. Upon co-treatment with ASC-CMed, SM22α expression was below detectable levels, irrespective of treatment (Figure 6, middle row panels). This indicates that ASC secrete factors that suppress SM22α in cytokine-stimulated HUVEC. The five-day pro-inflammatory activation of HUVEC induced hypertrophy as judged by F-actin detection with phalloidin staining (Figure 6, the lower row of panels). The hypertrophy was stronger and associated with transcellular stress fibres in HUVEC induced to undergo EndMT. Co-treatment with ASC-CMed, at least qualitatively, reduced the hypertrophy and intracellular stress fibres in HUVEC induced that underwent EndMT.

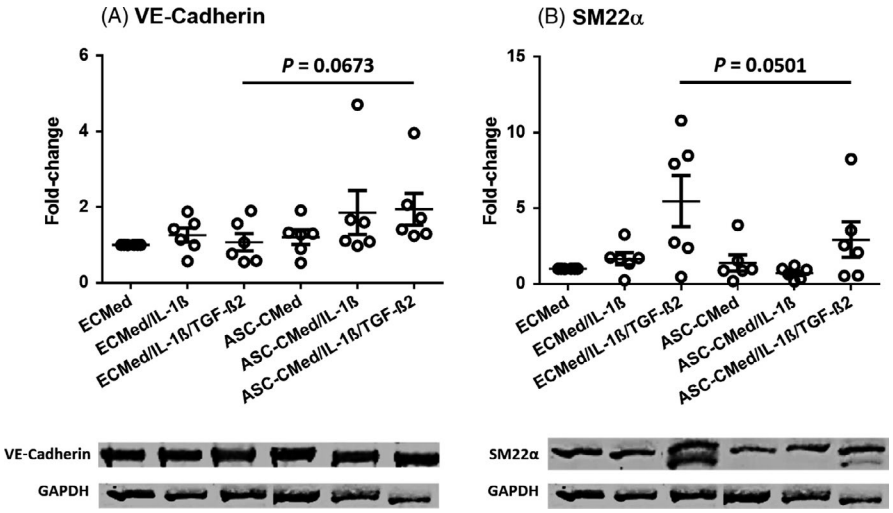

FIGURE 5 Protein expression of A, VE-cadherin and B, SM22α by Western blot of HUVEC under stimulation with IL-1β or co-stimulation with IL-1β/TGF-β2, both in ECMed and in ASC-CMed, for five days. Data were analysed by one-way ANOVA with Sidak's multiple comparison test for the groups ECMed/IL-1β/TGF-β2 vs ASC-CMed/IL-1β/TGF-β2; *P*-values for the Sidak's multiple comparison test are shown in the figure. Values represent mean ± SEM of 6 independent experiments

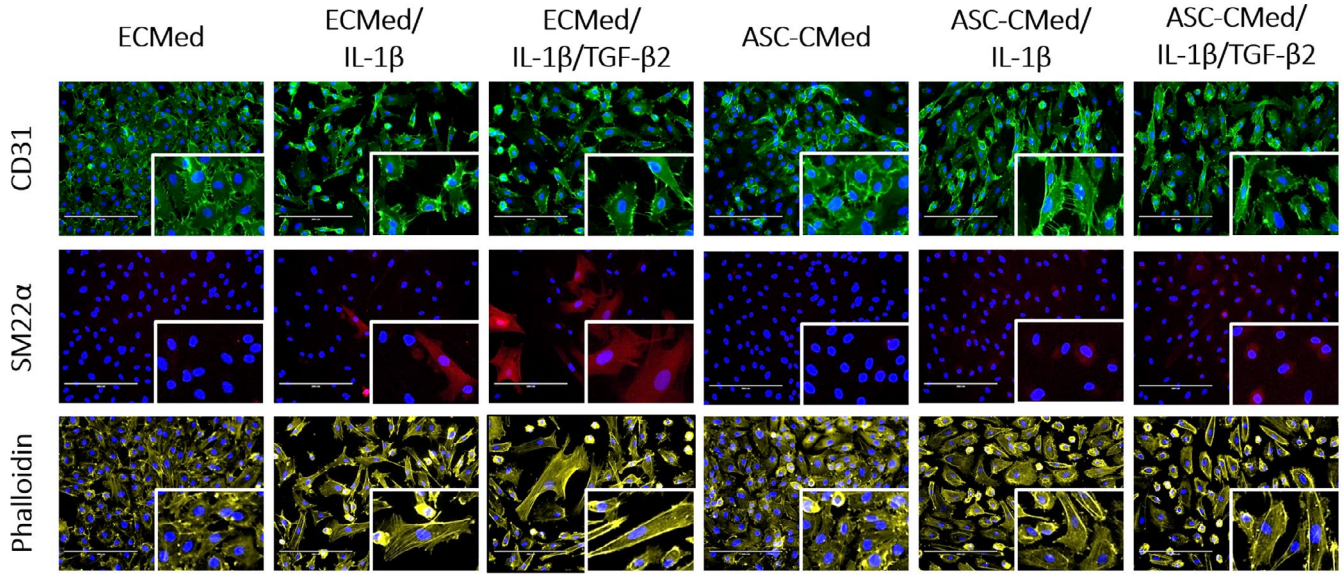

FIGURE 6 Fluorescence microscopy for phalloidin, SM22α, and CD31 of HUVEC after stimulation with IL-1β or co-stimulation with IL-1β/TGF-β2, both in ECMed and in ASC-CMed, for five days. Scale reference: 100 μm

Downstream TGF-ß signalling in EndMT is governed by the complex of the canonical TGF-β type II receptor (*TGFBR2*) and the TGF-β type I receptor ALK5 (*ALK5*) that activate any of the transcription factors Snail (*SNAI1*), Slug (*SNAI2*) or Twist (*TWIST1*). The expression of *TGFBR2* remained unchanged, irrespective of cytokine treatment or co-treatment with ASC-CMed (Figure S1 A). However, as we published before, *ALK5* expression increased upon stimulation of EndMT for five days, albeit not significantly (Figure S1 B). The co-treatment with ASC-CMed did not influence the expression of *ALK5* irrespective of cytokine treatment. Expression of the most relevant downstream EndMT-associated transcription factor *SNAI1* paralleled the expression pattern of *ALK5*, that is, upregulation by co-stimulation with IL-1β and TGF-β2, while ASC-CMed had no influence on its expression (Figure S1 C). The expression of the second relevant transcription factor *SNAI2* was unaffected except for treatment with both cytokines and the ASC-CMed (Figure S1 D, one-way ANOVA, $P = 0.0463$; Sidak's multiple comparison test, $P = 0.0244$). Expression of *TWIST1* was unchanged but tended to be upregulated in the presence of ASC-CMed (Figure S1 E).

3.5 | Factors secreted by ASC fail to restore impaired sprouting capacity of HUVEC undergoing EndMT

Endothelial cell function was assessed by short-term sprouting on Matrigel® and quantified through determination of nodes, segments, branches, total length, meshes and mean mesh size (Figure 7). Pro-inflammatory activated (5d, IL-1ß) HUVEC or HUVEC undergoing EndMT (5d, IL-1ß/TGF-ß2), largely lost their sprouting capacity, although this was more explicit in the latter group (Figure 7). Treatment with ASC-CMed did not restore the sprouting capacity of

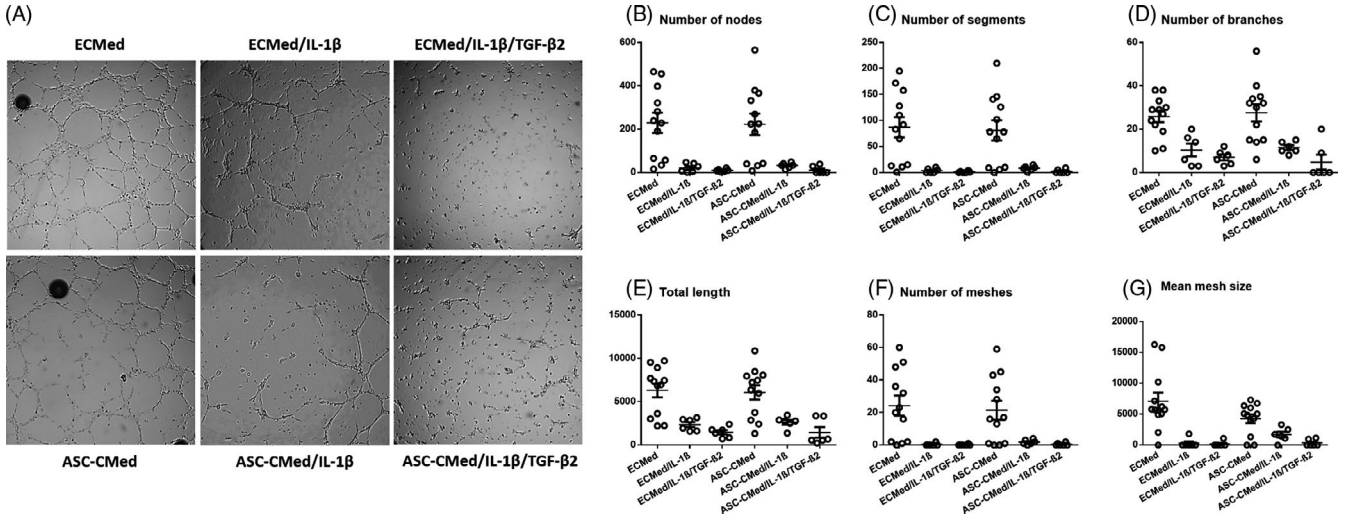

FIGURE 7 A, Sprouting assay (8 h) of HUVEC under stimulation with IL-1β or co-stimulation with IL-1β/TGF-β2, both in ECMed and in ASC-CMed, for five days. Brightfield microscopy, augmentation 2.5X. Quantification of B, number of nodes, C, number of segments, D, number of branches, E, number of meshes, F, total length and G, mean mesh size. Values represent mean ± SEM of three independent experiments in duplicate

HUVEC, while control treatment of HUVEC with ASC-CMed did not influence sprouting.

4 | DISCUSSION

The aim of our investigation was to assess the impact of factors secreted by ASC on EndMT induced by co-stimulation with IL-1β and TGF-β2. The main result is that ASC-CMed normalized or even promoted endothelial markers after EndMT induction, while constructive mesenchymal markers were suppressed. However, these ASC-secreted factors could not rescue the compromised endothelial functional phenotype because EC remained pro-inflammatory activated and had severely blunted sprouting capacity. Thus, the treatment of pro-inflammatory and pro-fibrotic-induced EndMT in vivo, such as during cardiac fibrosis, likely does not prevent endothelial dysfunction but might delay or suppress the mesenchymal transition itself, while more distant from a lesion ASC may still augment vascularization.

EndMT has been shown as an important process for the generation of myofibroblasts and, thus, fibrosis.[3] The potential of ASC to inhibit EndMT may be one of the mechanisms involved in myocardial regeneration following cell therapies based on ASC.[34-38,41] Literature supports that growth factors known to be secreted by ASC—such as FGF and VEGF [53,54]—could block EndMT.[55-57] Besides growth factors, the ASC secretome comprises microRNAs (often secluded in exosomes), among which are miR-155, miR-31, and miR-21, all known regulators of EndMT.[16,58,59] Another mechanism that may influence the expression of SM22α is an epigenetic modification, for instance, the trimethylation of histone three (H3K27me3) by enhancer of zeste homolog 2 (EZH2)[30]

Previously, mesenchymal cells derived from menstrual blood (MMC) were shown to ameliorate cardiac fibrosis via inhibition of EndMT in myocardial infarction.[60] The authors showed that the total number of cells co-expressing CD31 and αSMA in the infarcted heart was reduced from 30% in the control group to 20% in the group treated with MMC. In our in vitro study, we also showed that the inhibition of EndMT occurred in a limited manner, corroborating the findings of the in vivo study, which showed the complete blockage of the EndMT process could not be achieved in vivo. The percentage of cells co-expressing endothelial and mesenchymal markers in the sham group, as a reference, was less than 4% (compared to the 20% in the group treated with MMC), but even with the moderate reduction evidenced in the treated group, modulation of cardiac damage could be demonstrated by the reduction in the infarcted area. The use of ASC, in turn, was demonstrated to inhibit epithelial-to-mesenchymal transition (EMT) and consequently renal fibrosis.[61,62] Analogously to EndMT, EMT is a fibrotic process induced by TGF-β and mediated by key transcription factors such as Smad2/3, Snail and Twist.[63,64] The effects demonstrated with the use of ASC in EMT are an important indicator that these cells would also play a role in EndMT; thus, our findings on endothelial cells are also in agreement with the findings described for epithelial cells.

The detailed underlying molecular mechanism of EndMT blockage was not dissected in the present study. We expected a decrease in *SNAI1*, *SNAI2* and *TWIST1* expression after use of ASC-CMed because these are transcription factors involved in TGF-β–induced EndMT.[25,65] In contrast, we found that *SNAI2* was overexpressed when HUVEC co-stimulated with IL-1β/TGF-β2 were cultured in ASC-CMed, while no differences were found for *SNAI1* or *TWIST1*. Still, it was described in the literature that although EndMT is associated with an increased expression of *SNAI2*, the overexpression of *SNAI2* alone is not enough to promote EndMT, being also required the inhibition of the *SNAI2* inhibitor GSK-3β.[23] The GSK-3β, in turn, is inhibited by Smad2/3,[66] which is recruited by TGF-β.[67] Thus, in the hypothesis that ASC-CMed

would interrupt the canonical TGF-β pathway, Smad2/3 would be decreased and GSK-3β would not be inhibited, consequently blocking the SNAI2. Still, besides the predominant TGF-β canonical pathway, the non-canonical pathway was also described as mediating EndMT.[68,69] Other mechanisms involve the AKT signalling pathway, via the FOXO3 transcription factor,[70-72] and the MAPK/ERK pathway, via the ELK1 transcription factor.[28] Besides these pathways, the study of exosomes and miRNAs has emerged in the past few years, showing the presence of several entities involved in the EndMT process, such as mi21, mi146, let7 [12,72,73]

5 | CONCLUSION

The present study supports the anti-fibrotic effects of ASC-CMed through the modulation of the endothelial-mesenchymal transition process. We demonstrated that ASC-CMed reduces EndMT induced by co-stimulation with IL-1β and TGF-β2 as evidenced by the reduction in expression of mesenchymal markers. Still, further investigations are needed to elucidate the exact underlying mechanisms.

ACKNOWLEDGEMENTS

The authors would like to express their very great appreciation for the assistance provided by Henk Moorlag for the isolation and culture of human umbilical vein endothelial cells (HUVEC).

CONFLICT OF INTEREST

The authors declare no conflicts of interest.

AUTHOR CONTRIBUTION

TTAL has contributed to the conception and design of the work, data collection, data analysis and interpretation, drafting the article, critical revision of the article and final approval of the manuscript text. GRL has contributed to the conception and design of the work, data collection, data analysis and interpretation, drafting the article, critical revision of the article and final approval of the manuscript text. LFPM has contributed to the data analysis and interpretation, critical revision of the article and final approval of the manuscript text. MCH has contributed to the conception and design of the work, data analysis and interpretation, critical revision of the article and final approval of the manuscript text.

ORCID

Tácia Tavares Aquinas Liguori https://orcid.org/0000-0002-4150-3144

Gabriel Romero Liguori https://orcid.org/0000-0002-8089-1477

REFERENCES

1. Bui AL, Horwich TB, Fonarow GC. Epidemiology and risk profile of heart failure. *Nat Rev Cardiol*. 2011;8(1):30-41.
2. Howard CM, Baudino TA. Dynamic cell-cell and cell-ECM interactions in the heart. *J Mol Cell Cardiol*. 2014;70:19-26.
3. Kong P, Christia P, Frangogiannis NG. The pathogenesis of cardiac fibrosis. *Cell Mol Life Sci*. 2014;71(4):549-574.
4. Travers JG, Kamal FA, Robbins J, Yutzey KE, Blaxall BC. Cardiac Fibrosis: The Fibroblast Awakens. *Circ Res*. 2016;118(6):1021-1040.
5. Krenning G, Zeisberg EM, Kalluri R. The origin of fibroblasts and mechanism of cardiac fibrosis. *J Cell Physiol*. 2010;225(3):631-637.
6. Krenning G, Barauna VG, Krieger JE, Harmsen MC, Moonen J-R. Endothelial Plasticity: Shifting Phenotypes through Force Feedback. *Stem Cells Int*. 2016;2016:9762959.
7. Souilhol C, Harmsen MC, Evans PC, Krenning G. Endothelial-mesenchymal transition in atherosclerosis. *Cardiovasc Res*. 2018;114(4):565-577.
8. Aisagbonhi O, Rai M, Ryzhov S, Atria N, Feoktistov I, Hatzopoulos AK. Experimental myocardial infarction triggers canonical Wnt signaling and endothelial-to-mesenchymal transition. *Dis Model Mech*. 2011;4(4):469-483.
9. Boyer AS, Ayerinskas II, Vincent EB, McKinney LA, Weeks DL, Runyan RB. TGFbeta2 and TGFbeta3 have separate and sequential activities during epithelial-mesenchymal cell transformation in the embryonic heart. *Dev Biol*. 1999;208(2):530-545.
10. Moonen J-R, Lee ES, Schmidt M, et al. Endothelial-to-mesenchymal transition contributes to fibro-proliferative vascular disease and is modulated by fluid shear stress. *Cardiovasc Res*. 2015;108(3):377-386.
11. Zeisberg EM, Tarnavski O, Zeisberg M, et al. Endothelial-to-mesenchymal transition contributes to cardiac fibrosis. *Nat Med*. 2007;13(8):952-961.
12. Ghosh AK, Nagpal V, Covington JW, Michaels MA, Vaughan DE. Molecular basis of cardiac endothelial-to-mesenchymal transition (EndMT): differential expression of microRNAs during EndMT. *Cell Signal*. 2012;24(5):1031-1036.
13. Kim J, Kim J, Lee SH, et al. Cytokine-Like 1 regulates cardiac fibrosis via modulation of TGF-β signaling. *PLoS ONE*. 2016;11(11):e0166480.
14. Feng B, Cao Y, Chen S, Chu X, Chu Y, Chakrabarti S. miR-200b mediates endothelial-to-mesenchymal transition in diabetic cardiomyopathy. *Diabetes*. 2016;65(3):768-779.
15. Tang R-N, Lv L-L, Zhang J-D, et al. Effects of angiotensin II receptor blocker on myocardial endothelial-to-mesenchymal transition in diabetic rats. *Int J Cardiol*. 2013;162(2):92-99.
16. Kumarswamy R, Volkmann I, Jazbutyte V, Dangwal S, Park D-H, Thum T. Transforming growth factor-β-induced endothelial-to-mesenchymal transition is partly mediated by microRNA-21. *Arterioscler Thromb Vasc Biol*. 2012;32(2):361-369.
17. Medici D. Endothelial-Mesenchymal Transition in Regenerative Medicine. *Stem Cells Int*. 2016;2016:1–7.
18. Piera-Velazquez S, Mendoza FA, Jimenez SA. Endothelial to Mesenchymal Transition (EndoMT) in the Pathogenesis of Human Fibrotic Diseases. *J Clin Med Res*. 2016;5(4):45.
19. Yoshimatsu Y, Watabe T. Roles of TGF-β signals in endothelial-mesenchymal transition during cardiac fibrosis. *Int J Inflam*. 2011;2011:724080.
20. Piera-Velazquez S, Li Z, Jimenez SA. Role of endothelial-mesenchymal transition (EndoMT) in the pathogenesis of fibrotic disorders. *Am J Pathol*. 2011;179(3):1074-1080.
21. Gordon KJ, Blobe GC. Role of transforming growth factor-β superfamily signaling pathways in human disease. *Biochimica et Biophysica. Acta (BBA) - Mol Basis Dis*. 2008;1782(4):197-228.

22. Maring JA, van Meeteren LA, Goumans MJ, ten Dijke P. Interrogating TGF-β Function and Regulation in Endothelial Cells. *Methods Mol Biol*. 2016;193-203.
23. Medici D, Potenta S, Kalluri R. Transforming Growth Factor-β2 promotes Snail-mediated endothelial-mesenchymal transition through convergence of Smad-dependent and Smad-independent signaling. *Biochem J*. 2011;437(3):515.
24. Li C, Dong F, Jia Y, et al. Notch signal regulates corneal endothelial-to-mesenchymal transition. *Am J Pathol*. 2013;183(3):786-795.
25. Kokudo T, Suzuki Y, Yoshimatsu Y, Yamazaki T, Watabe T, Miyazono K. Snail is required for TGFbeta-induced endothelial-mesenchymal transition of embryonic stem cell-derived endothelial cells. *J Cell Sci*. 2008;121(Pt 20):3317-3324.
26. Zeng L, Wang G, Ummarino D, et al. Histone deacetylase 3 unconventional splicing mediates endothelial-to-mesenchymal transition through transforming growth factor β2. *J Biol Chem*. 2013;288(44):31853-31866.
27. Feng J, Zhang J, Jackson AO, et al. Apolipoprotein A1 Inhibits the TGF-β1-induced endothelial-to-mesenchymal transition of human coronary artery endothelial cells. *Cardiology*. 2017;137(3):179-187.
28. Suzuki HI, Katsura A, Mihira H, Horie M, Saito A, Miyazono K. Regulation of TGF-β-mediated endothelial-mesenchymal transition by microRNA-27. *J Biochem*. 2017;161(5):417-420.
29. Maleszewska M, Moonen J-R, Huijkman N, van de Sluis B, Krenning G, Harmsen MC. IL-1β and TGFβ2 synergistically induce endothelial to mesenchymal transition in an NFκB-dependent manner. *Immunobiology*. 2013;218(4):443-454.
30. Maleszewska M, Gjaltema R, Krenning G, Harmsen MC. Enhancer of zeste homolog-2 (EZH2) methyltransferase regulates transgelin/smooth muscle-22α expression in endothelial cells in response to interleukin-1β and transforming growth factor-β2. *Cell Signal*. 2015;27(8):1589-1596.
31. Lee ES, Boldo LS, Fernandez BO, Feelisch M, Harmsen MC. Suppression of TAK1 pathway by shear stress counteracts the inflammatory endothelial cell phenotype induced by oxidative stress and TGF-β1. *Sci Rep*. 2017;7:42487.
32. Montorfano I, Becerra A, Cerro R, et al. Oxidative stress mediates the conversion of endothelial cells into myofibroblasts via a TGF-β1 and TGF-β2-dependent pathway. *Lab Invest*. 2014;94(10):1068-1082.
33. Richter K, Konzack A, Pihlajaniemi T, Heljasvaara R, Kietzmann T. Redox-fibrosis: Impact of TGFβ1 on ROS generators, mediators and functional consequences. *Redox Biol*. 2015;6:344-352.
34. Mazo M, Hernández S, Gavira JJ, et al. Treatment of Reperfused Ischemia With Adipose-Derived Stem Cells in a Preclinical Swine Model of Myocardial Infarction. *Cell Transplant*. 2012;21(12):2723-2733.
35. Yu LH, Kim MH, Park TH, et al. Improvement of cardiac function and remodeling by transplanting adipose tissue-derived stromal cells into a mouse model of acute myocardial infarction. *Int J Cardiol*. 2010;139(2):166-172.
36. Perin EC, Sanz-Ruiz R, Sánchez PL, et al. Adipose-derived regenerative cells in patients with ischemic cardiomyopathy: The PRECISE Trial. *Am Heart J*. 2014;168(1):88-95.e2.
37. Mazo M, Planat-Bénard V, Abizanda G, et al. Transplantation of adipose derived stromal cells is associated with functional improvement in a rat model of chronic myocardial infarction. *Eur J Heart Fail*. 2008;10(5):454-462.
38. Przybyt E, Harmsen MC. Mesenchymal Stem Cells: Promising for Myocardial Regeneration? *Curr Stem Cell Res Ther*. 2013;8(4):270-277.
39. ten Sande JN, Smit NW, Parvizi M, et al. Differential Mechanisms of Myocardial Conduction Slowing by Adipose Tissue-Derived Stromal Cells Derived from Different Species. *Stem Cells Transl Med*. 2017;6(1):22-30.
40. Tano N, Narita T, Kaneko M, et al. Epicardial placement of mesenchymal stromal cell-sheets for the treatment of ischemic cardiomyopathy; in vivo proof-of-concept study. *Mol Ther*. 2014;22(10):1864-1871.
41. Hamdi H, Boitard SE, Planat-Benard V, et al. Efficacy of epicardially delivered adipose stroma cell sheets in dilated cardiomyopathy. *Cardiovasc Res*. 2013;99(4):640-647.
42. Araña M, Gavira JJ, Peña E, et al. Epicardial delivery of collagen patches with adipose-derived stem cells in rat and minipig models of chronic myocardial infarction. *Biomaterials*. 2014;35(1):143-151.
43. He J, Cai Y, Luo LM, Liu HB. Hypoxic adipose mesenchymal stem cells derived conditioned medium protects myocardial infarct in rat. *Eur Rev Med Pharmacol Sci*. 2015;19(22):4397-4406.
44. Jiang Y, Chang P, Pei YU, et al. Intramyocardial injection of hypoxia-preconditioned adipose-derived stromal cells treats acute myocardial infarction: an in vivo study in swine. *Cell Tissue Res*. 2014;358(2):417-432.
45. Spiekman M, Przybyt E, Plantinga JA, Gibbs S, van der Lei B, Harmsen MC. Adipose tissue-derived stromal cells inhibit TGF-β1-induced differentiation of human dermal fibroblasts and keloid scar-derived fibroblasts in a paracrine fashion. *Plast Reconstr Surg*. 2014;134(4):699-712.
46. Zvonic S, Lefevre M, Kilroy G, et al. Secretome of primary cultures of human adipose-derived stem cells: modulation of serpins by adipogenesis. *Mol Cell Proteomics*. 2007;6(1):18-28.
47. Kapur SK, Katz AJ. Review of the adipose derived stem cell secretome. *Biochimie*. 2013;95(12):2222-2228.
48. Kalinina N, Kharlampieva D, Loguinova M, et al. Characterization of secretomes provides evidence for adipose-derived mesenchymal stromal cells subtypes. *Stem Cell Res Ther*. 2015;6:221.
49. Przybyt E, Krenning G, Brinker M, Harmsen MC. Adipose stromal cells primed with hypoxia and inflammation enhance cardiomyocyte proliferation rate in vitro through STAT3 and Erk1/2. *J Transl Med*. 2013;11:39.
50. Mert T, Kurt AH, Arslan M, Çelik A, Tugtag B, Akkurt A. Anti-inflammatory and Anti-nociceptive Actions of Systemically or Locally Treated Adipose-Derived Mesenchymal Stem Cells in Experimental Inflammatory Model. *Inflammation*. 2015;38(3):1302-1310.
51. Tuin A, Kluijtmans SG, Bouwstra JB, Harmsen MC, Van Luyn M. Recombinant gelatin microspheres: novel formulations for tissue repair? *Tissue Eng Part A*. 2010;16(6):1811-1821.
52. Parvizi M, Bolhuis-Versteeg L, Poot AA, Harmsen MC. Efficient generation of smooth muscle cells from adipose-derived stromal cells by 3D mechanical stimulation can substitute the use of growth factors in vascular tissue engineering. *Biotechnol J*. 2016;11(7):932-944.
53. An H-Y, Shin H-S, Choi J-S, Kim HJ, Lim J-Y, Kim Y-M. Adipose Mesenchymal Stem Cell Secretome Modulated in Hypoxia for Remodeling of Radiation-Induced Salivary Gland Damage. *PLoS ONE*. 2015;10(11):e0141862.
54. Lee CS, Burnsed OA, Raghuram V, Kalisvaart J, Boyan BD, Schwartz Z. Adipose stem cells can secrete angiogenic factors that inhibit hyaline cartilage regeneration. *Stem Cell Res Ther*. 2012;3(4):35.
55. Illigens BM-W, Casar Berazaluce A, Poutias D, Gasser R, DelNido PJ, Friehs I. Vascular endothelial growth factor prevents endothelial-to-mesenchymal transition in hypertrophy. *Ann Thorac Surg*. 2017;104(3):932-939.
56. Chen P-Y, Qin L, Barnes C, et al. FGF regulates TGF-β signaling and endothelial-to-mesenchymal transition via control of let-7 miRNA expression. *Cell Rep*. 2012;2(6):1684-1696.
57. Correia A, Moonen J-R, Brinker M, Krenning G. FGF2 inhibits endothelial-mesenchymal transition through microRNA-20a-mediated repression of canonical TGF-β signaling. *J Cell Sci*. 2016;129(3):569-579.

58. Bijkerk R, G. de Bruin R, van Solingen C, et al. MicroRNA-155 functions as a negative regulator of RhoA signaling in TGF-β-induced endothelial to mesenchymal transition. *Microrna*. 2012;1(1):2-10.
59. Katsura A, Suzuki HI, Ueno T, et al. MicroRNA-31 is a positive modulator of endothelial-mesenchymal transition and associated secretory phenotype induced by TGF-β. *Genes Cells*. 2016;21(1):99-116.
60. Zhang Z, Wang J-A, Xu Y, et al. Menstrual blood derived mesenchymal cells ameliorate cardiac fibrosis via inhibition of endothelial to mesenchymal transition in myocardial infarction. *Int J Cardiol*. 2013;168(2):1711-1714.
61. Donizetti-Oliveira C, Semedo P, Burgos-Silva M, et al. Adipose tissue-derived stem cell treatment prevents renal disease progression. *Cell Transplant*. 2012;21(8):1727-1741.
62. Song Y, Peng C, Lv S, et al. Adipose-derived stem cells ameliorate renal interstitial fibrosis through inhibition of EMT and inflammatory response via TGF-β1 signaling pathway. *Int Immunopharmacol*. 2017;44:115-122.
63. Lamouille S, Xu J, Derynck R. Molecular mechanisms of epithelial–mesenchymal transition. *Nat Rev Mol Cell Biol*. 2014;15(3):178-196.
64. Luna-Zurita L, Prados B, Grego-Bessa J, et al. Integration of a Notch-dependent mesenchymal gene program and Bmp2-driven cell invasiveness regulates murine cardiac valve formation. *J Clin Invest*. 2010;120(10):3493-3507.
65. Medici D, Potenta S, Kalluri R. Transforming growth factor-β2 promotes Snail-mediated endothelial–mesenchymal transition through convergence of Smad-dependent and Smad-independent signalling. *Biochem J*. 2011;437(3):515-520.
66. Aragon E, Goerner N, Zaromytidou A-I, et al. A Smad action turnover switch operated by WW domain readers of a phosphoserine code. *Genes Dev*. 2011;25(12):1275-1288.
67. Zi Z, Chapnick DA, Liu X. Dynamics of TGF-β/Smad signaling. *FEBS Lett*. 2012;586(14):1921-1928.
68. Chang A, Fu YangXin, Garside V, et al. Notch initiates the endothelial-to-mesenchymal transition in the atrioventricular canal through autocrine activation of soluble guanylyl cyclase. *Dev Cell*. 2011;21(2):288-300.
69. Cho JG, Lee A, Chang W, Lee M-S, Kim J. Endothelial to Mesenchymal Transition Represents a Key Link in the Interaction between Inflammation and Endothelial Dysfunction. *Front Immunol*. 2018;9:294.
70. Zhang Z, Zhang T, Zhou Y, et al. Activated phosphatidylinositol 3-kinase/Akt inhibits the transition of endothelial progenitor cells to mesenchymal cells by regulating the forkhead box subgroup O-3a signaling. *Cell Physiol Biochem*. 2015;35(4):1643-1653.
71. Zhang J, Zhang Z, Zhang DY, Zhu J, Zhang T, Wang C. microRNA 126 inhibits the transition of endothelial progenitor cells to mesenchymal cells via the PIK3R2-PI3K/Akt signalling pathway. *PLoS ONE*. 2013;8(12):e83294.
72. Kumarswamy R, Volkmann I, Jazbutyte V, Dangwal S, Park D-H, Thum T. Transforming Growth Factor-β–Induced Endothelial-to-Mesenchymal Transition Is Partly Mediated by MicroRNA-21. *Arterioscler Thromb Vasc Biol*. 2012;32(2):361-369.
73. Baglio SR, Rooijers K, Koppers-Lalic D, et al. Human bone marrow- and adipose-mesenchymal stem cells secrete exosomes enriched in distinctive miRNA and tRNA species. *Stem Cell Res Ther*. 2015;6:127.

SUPPORTING INFORMATION

Additional supporting information may be found online in the Supporting Information section at the end of the article.

How to cite this article: Liguori TTA, Liguori GR, Pinho Moreira LF, Harmsen MC. Adipose tissue–derived stromal cells' conditioned medium modulates endothelial-mesenchymal transition induced by IL-1β/TGF-β2 but does not restore endothelial function. *Cell Prolif*. 2019;52:e12629. https://doi.org/10.1111/cpr.12629